

OPEN ACCESS

How flat is your detector? Non-uniform annular detector sensitivity in STEM quantification

To cite this article: K E MacArthur *et al* 2014 *J. Phys.: Conf. Ser.* **522** 012018

View the [article online](#) for updates and enhancements.

You may also like

- [Information travels in massless fields in 1+1 dimensions where energy cannot](#)
Robert H Jonsson
- [Transmitting qubits through relativistic fields](#)
Robert H Jonsson, Katja Ried, Eduardo Martín-Martínez *et al.*
- [Comparing performances of a CdTe X-ray spectroscopic detector and an X-ray dual-energy sandwich detector](#)
A Gorecki, A Brambilla, V Moulin *et al.*



ECS
The
Electrochemical
Society
Advancing solid state &
electrochemical science & technology

DISCOVER
how sustainability
intersects with
electrochemistry & solid
state science research

How flat is your detector? Non-uniform annular detector sensitivity in STEM quantification

K E MacArthur¹, L B Jones, P D Nellist

Department of Materials, University of Oxford, Parks Road Oxford OX1 3PH, UK

E-mail: katherine.macarthur@materials.ox.ac.uk

Abstract. Recording HAADF STEM data on an absolute scale for image quantification is becoming increasingly common. A particular challenge with this method is that most image simulation programs model the detector as being circularly symmetric and exhibiting uniform detection sensitivity across its entire active region. For a real detector this is rarely the case; it then becomes vital to understand how far one's detector deviates from the ideal. Here we investigate a collection of detector maps recorded using hardware from each of the current major manufacturers. Using these maps we compare their different asymmetries and any non-uniformities in their sensitivity. To facilitate this we define the parameters; 'flatness', 'roundness', 'smoothness' and 'ellipticity', evaluate each hardware with respect to these and rank them.

1. Introduction

Quantification of high-angle annular dark-field scanning transmission electron microscopy (HAADF STEM) data has been growing in interest in recent years [1,2]. Typically the images (recorded in counts) are normalised by the count-rate equivalent to the entire STEM probe being incident on the detector. This detector calibration for HAADF STEM requires the beam to be rastered over the detector to produce a 'detector map'. This map then yields both the number of counts in the detector hole (vacuum level - equivalent to the D.C. offset) and the gain of the amplifying electronics, also referred to as detector sensitivity. Knowing this offset and gain, the data can then be expressed as a fraction of the incident beam intensity, by simply subtracting the D.C. offset and dividing by the gain, facilitating direct comparison with image simulations. The scaled images can then be expressed in units of 'fractional beam intensity' allowing for local variation in sample composition to be observed, when thickness is known[3], or variations in thickness to be measured where composition is fixed[4].

A particular challenge with this method is that most image simulation programs model the detector as being circularly symmetric and exhibiting uniform detection sensitivity across its entire active region[5]. Here we investigate a collection of detector maps recorded using hardware from each of the current major manufactures. Working from the premise that no detector is ideal or uniform we set out to characterise how asymmetric and non-uniform these detectors are in their response. To facilitate this we define the parameters; 'flatness', 'roundness', 'smoothness' and 'ellipticity', evaluate each hardware with respect to these and rank them. We also present some important methodological

¹ To whom any correspondence should be addressed.

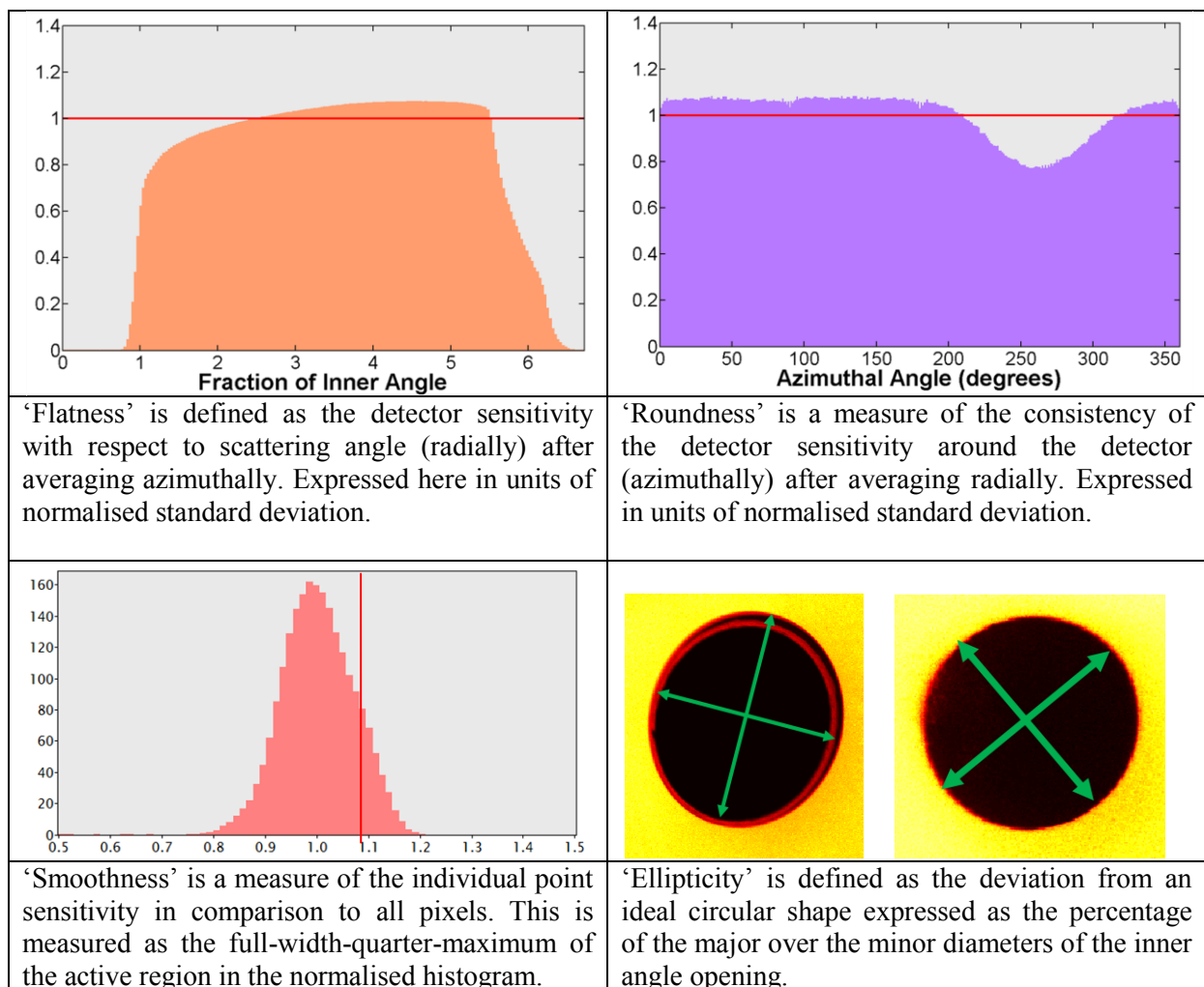


subtleties in the mapping procedure including sample occlusion, detector saturation and map-distortion resulting from post-specimen optics. Considering all these parameters and effects we show how any detector or mapping-method deficiencies can contribute to errors in experimental image quantification.

2. Method

To determine the dark-field ‘count-rate’ that corresponds to 100% of the STEM probe’s current one must first map the detector’s sensitivity. This map is produced by forming focused probe at the detector plane either, for example using a confocal or diffractive mode, which is then rastered across the detector. The integrated ADF signal is read out with probe position, similar to acquiring a normal STEM image, to produce the sensitivity map. If the probe current used for imaging would saturate or damage the detector, then it is acceptable to drop the current by a known ratio by adjusting the mapping dwell time or probe forming aperture size (amplifier brightness and contrast settings must remain unchanged between mapping and imaging).

These maps allow the entire visible surface of detectors to be inspected and analysed for their symmetry and manufacturing quality. All the comparisons derived in this paper are directly from the detector maps shown, Figure 1, relying on the following definitions:



Finally, the angle ratio is simply defined as the outer angle divided by the inner angle.

3. Results and Discussion

The definitions described above were applied to each of the six detector maps, the results of which are summarised below. For all parameters, apart from the angle ratio, the value present in the table is the measure of deviation from the ideal cases; therefore a larger number means a more asymmetric detector. To calculate the final value for ranking an arithmetic average was carried out of all the parameters, except angle ratio.

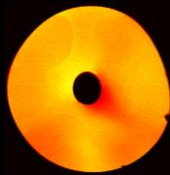
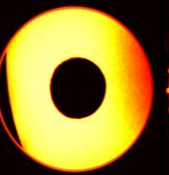
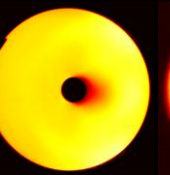
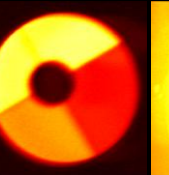
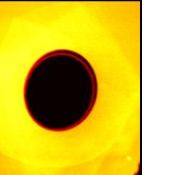
Manufacturer	Company 1			Company 2	Company 3	Company 4
	Detector A	Detector B	Detector C	Detector D	Detector E	Detector F
Detector Map						
Angle Ratio	5.47 x	3.09 x	2.89 x	5.91 x	2.90 x	3.50 x
'Flatness'	8.9 %	6.8 %	24.9 %	10.4 %	9.7 %	14.5 %
'Roundness'	8.2 %	5.4 %	10.6 %	5.4 %	28.1 %	2.4 %
'Smoothness'	30.0 % *	15.1 %	16.3 %	18.0 %	87.2 %	23.2 % *
'Ellipticity'	19.6 %	4.8 %	8.9 %	0.5 %	4.3 %	13.3 %
Average	16.7 %	8.0 %	15.2 %	8.6 %	32.3 %	13.4 %

Figure 1. Scaled sensitivity images of the six detectors studied, grouped by manufacturer. For each type of non-uniformity, the percentage deviation from perfection is shown. For each performance metric the most uniform detector is highlighted in bold. Lastly, an overall “non-uniformity” score is tabulated.

As well as the hardware effects already compared there are several alignment and methodology factors, present in the maps above, which will also greatly affect quantification methods. Firstly, the map of detector A demonstrated two main problems; sample occlusion and post specimen optics. The presence of any sample, in this cases holey carbon film, has the potential to disturb or distort the beam during the map and will also affect the gain measurement used for later quantifications. The post specimen optics effect is apparent from the 3-fold symmetrical distortion present in the map, resulting from the post-specimen hexapole correctors present in the TEM/STEM system. The corrector lenses will not only affect the detector map but will also distort, thereby providing radial non-uniformity to, the electron flux the detector will see during imaging.

Secondly detector F demonstrates evidence of ‘burn in’ from saturation. This is due the detector being saturated with too large a dose of current prior to the map being acquired at a lower current level. The image therefore contains residual counts which will affect quantification results by increasing the average detector sensitivity measured.

Lastly detector E demonstrates an example of a quadrant detector. This necessitates four separate readouts and therefore four separate amplifying electronics. In this example the quadrants have not been properly gain normalised during the experiment, resulting in such an intensity variation in the final detector map. With correct normalisation between the quadrants, however, it is possible to combat some of the hardware imbalances.

4. Conclusion

- The largest detector, physically, is detector D with the maximum angle ratio, providing signal to noise benefits from collecting over a greater range of angles.
- The flattest detector is Detector B. This detector will collect scattering to different angles most fairly and will be the most accurate for composition mapping studies.
- The roundest detector is Detector F. This detector would be the best for avoiding imaging artefacts such as small shifts in column positions.
- The smoothest detector is Detector B, suggesting it may have the best manufacturing quality.
- The least elliptical detector is Detector D. This is essential for accurate inner-angle measurement for reliable comparison with simulation.
- The largest collection-angle range detector (inner- to outer-angle ratio) is Detector D. For a fixed inner-angle this larger ratio means a bigger outer-angle and improved total electron collection giving the best signal to noise ratio possible.

We have also demonstrated the importance of mapping procedure in the quantification process.

5. References

- [1] A. Singhal, J. Yang, J. Gibson, *Ultramicroscopy* 67 (1997) 191–206.
- [2] J.M. Lebeau, S. Stemmer, *Ultramicroscopy* 108 (2008) 1653–1658.
- [3] A. Rosenauer, T. Mehrtens, K. Müller, K. Gries, M. Schowalter, P.V. Satyam, S. Bley, C. Tessarek, D. Hommel, K. Sebald, M. Seyfried, J. Gutowski, A. Avramescu, K. Engl, S. Lutgen, *Ultramicroscopy* 111 (2011) 1316–27.
- [4] H. Katz-Boon, C.J. Rossouw, C. Dwyer, J. Etheridge, *Ultramicroscopy* 124C (2012) 61–70.
- [5] S.D. Findlay, J.M. LeBeau, *Ultramicroscopy* 124 (2013) 52–60.

6. Acknowledgments

The authors gratefully acknowledge Dr Dogan Ozkaya, Johnson-Matthey, Dr Tim Pennycook, SuperSTEM Laboratory, and Dr Armand Béch e, EMAT Antwerp, for their help in acquiring detector maps. They would also like to thank EPSRC and Johnson-Matthey for their financial support. The research leading to these results has received funding from the European Union Seventh Framework Programme under Grant Agreement 312483 - ESTEEM2 (Integrated Infrastructure Initiative–I3).